Low ΔT_j Stress Cycle Effect in IGBT Power Module Die-Attach Lifetime Modeling

Wei Lai, Minyou Chen, *Senior Member, IEEE*, Li Ran, *Senior Member, IEEE*, Olayiwola Alatise, *Member, IEEE*, Shengyou Xu, and Philip Mawby, *Senior Member, IEEE*

***Abstract*—Operational management for reliability of power electronic converters requires sensitive condition monitoring and accurate lifetime modeling. This study adds to the second aspect by examining the effect of cyclic junction temperature variations ΔT_j of low amplitude in different stages of the power module ageing process. It is found that such relatively minor stress cycles, which happen frequently during normal operation, may not be able to directly initiate a crack but can contribute to the development of damage due to stress concentration. This agrees with the observation that the ageing process tends to accelerate toward the end of life. This study investigates the dependence of the ageing effect on the amplitude of ΔT_j, the mean junction temperature T_m, and the present health condition of the module, and proposes a lifetime model focusing on die-attach solder fatigue. It is assumed that the future-ageing process is independent of the operational history that has led to the current state of health. The model is intended for operational management of converter systems that are subjected to frequent low ΔT_j stress cycles and are supposed to be in service reliably for a long time with a slow ageing process. Experimental results validate the model.**

***Index Terms*—Lifetime modeling, low junction temperature cycling, power cycling, power module, reliability, solder fatigue.**

I. Introduction

INSULATED gate bipolar transistors (IGBTs) are the working horse in many power electronic systems, playing a key role in fast control and efficient power conversion. However, IGBT modules are also the more vulnerable components in the system [1], [2]. To support design and operational management, it is important to understand the effect of realistic stresses on the module and establish lifetime models.

Manuscript received July 14, 2015; revised September 26, 2015; accepted November 4, 2015. Date of publication November 18, 2015; date of current version March 25, 2016. This work was supported in part by the National Natural Science Foundation of China under Grant 51477019, by the National Basic Research Program of China under Grant 2012CB215205), by the Fundamental Research Funds for the Central Universities (106112015CDJXY150004), U.K. EPSRC funding through underpinning power electronics devices and components themes (EP/L007010/1 and EP/K034804/1), and by the National "111" Project (B08036). Recommended for publication by Associate Editor S. Mazumder.

W. Lai, M. Chen, and S. Xu are with the State Key Laboratory of Power Transmission Equipment and System Security and New Technology, School of Electrical Engineering, Chongqing University, Chongqing 400044, China (e-mail: laiweicqu@126.com; mchencqu@126.com; sheng_you_xu@163.com).

L. Ran is with the State Key Laboratory of Power Transmission Equipment & System Security and New Technology, School of Electrical Engineering, Chongqing University, Chongqing 400044, China. He is also with the School of Engineering, University of Warwick, Coventry CV4 7AL, U.K. (e-mail: L.Ran@warwick.ac.uk).

O. Alatise and P. Mawby are with the School of Engineering, University of Warwick, Coventry CV4 7AL, U.K. (e-mail: O.Alatise@warwick.ac.uk; p.a.mawby@warwick.ac.uk).

Color versions of one or more of the figures in this paper are available online at http://ieeexplore.ieee.org.

Digital Object Identifier 10.1109/TPEL.2015.2501540

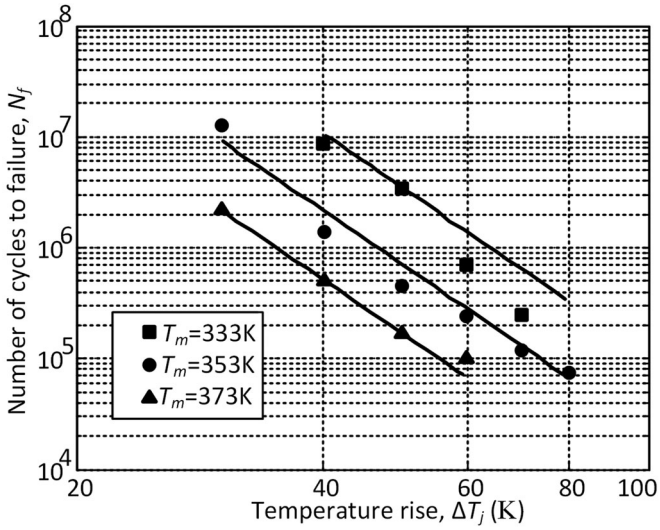

Fig. 1. Number of cycles to failure N_f as a function of ΔT_j and T_m.

A lifetime model is traditionally extracted from accelerated ageing tests under intensified stress conditions; the results are then extrapolated to the normal operation region of lesser stresses. For wire-bonded packaging, the root cause of the predominant failure mechanisms, i.e., solder pad fatigue and bond wire liftoff, is junction temperature cycling ΔT_j with the associated internal temperature gradient acting on the mismatch of coefficients of thermal expansion between different materials [3], [4]. Taken from [5], Fig. 1 shows the test results on an early design of 300-A/1200-V IGBT modules for a number of mean junction temperatures (T_m) and a range of ΔT_j amplitudes. More recent designs with improved reliability can only be tested in highly intensified stress conditions with, e.g., $\Delta T_j \geq 80$ K. This leads to uncertainty of extrapolation which has become a serious concern in the design and operational management of converters expected to work with minimum maintenance in environments that are difficult to access, e.g., in offshore wind turbines. The semiconductor power modules in a turbine converter typically need to survive $>5\times10^9$ temperature cycles of $\Delta T_j = 20 \sim 40$ K [6]–[8]. It is unrealistic to replicate the mission profile for the purpose of testing under such stress conditions of interest.

Bond wire joint and die-attach solder pad fatigues are the two ageing-to-failure mechanisms that have received most attention [9]–[12]. The authors in [13] show that the die-attach solder fatigue is usually more dominant, while bond wire joints start to degrade when the junction temperature is above 473 K. The authors in [14] show that cracks occur at the solder interfaces

between the die and bond wires when ΔT_j is over 100 K. As this study intends to further understand the effect of relatively low ΔT_j stress cycles, it will focus on die-attach solder fatigue although degraded bond wire joints could also be affected. It is assumed that the low ΔT_j stress cycles will not themselves cause initial cracks because a new module is generally designed to undergo elastic deformation in such conditions. The long-term effect of a large number of such minor stress cycles is predicted by extrapolation, and the effect is usually negligibly small in the presence of more severe stress cycles in the mission profile. However, there is strong evidence that the ageing process accelerates toward the end of life, and existing lifetime models based on linear superimposition cannot explain the phenomenon. It has been realized that stress concentration can happen at the crack tips in an aged solder pad. Once a crack is initiated, the effect of the small ΔT_j stress cycles may no longer be negligible. Therefore, it is necessary to examine the effect on aged modules.

This paper presents a new experimental scheme to compare the effect of the low ΔT_j stress cycles on aged and nonaged modules through power cycling. The variable junction-to-case thermal resistance $R_{\rm th}$ is used as an indication of the health condition of the power module; noticeable degradation is usually accompanied by an increase of $R_{\rm th}$ which can be measured externally. According to the results obtained from the aged power modules under different test conditions, the rates of thermal resistance increase are extracted. A new lifetime model is then proposed based on the changing characteristics of the thermal resistance in the ageing process. Section II presents the experiment methodology. Section III analyzes the assumption made and the structure proposed for the lifetime model which is developed more fully in Section IV. Section V concludes the paper.

II. Experimental Measurement of Low ΔT_j Stress Cycle Effect

A. Power Cycling Test Rig

The main electrical circuit for power cycling is shown in Fig. 2. Four IGBT modules (SKM50GB12T4, 50A/1200V) are connected in series to ensure that they are all subjected to the same cycling current. This type of module with a wire-bonded packaging structure as shown in Fig. 3 is used in all the tests of this study. There is one chip for each IGBT. Multiple samples are used to confirm the repeatability of the observed phenomena. A 100-mA current source is connected through all the modules which are permanently gated on. In this setup, a heating-up phase is initiated by closing the heating control switch. When the heating control switch later turns OFF, the IGBTs are sent into a cooling phase. The on-state power loss of the IGBT is dissipated as heat thereby causing a rise in the junction temperature. This change of the junction temperature causes temperature gradient and induces thermo-mechanical stresses between the silicon chip, the SnAg(3) solder and the copper substrate. The peak junction temperature of each IGBT module $(T_{j\max})$ is obtained by measuring the corresponding collector–emitter voltage $(V_{\rm CE})$ caused by the 100-mA current when the heating control switch is OFF. During cooling, the

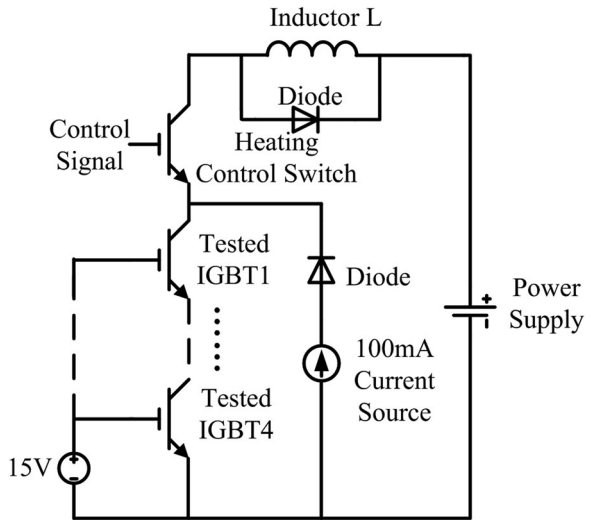

Fig. 2. Main circuit.

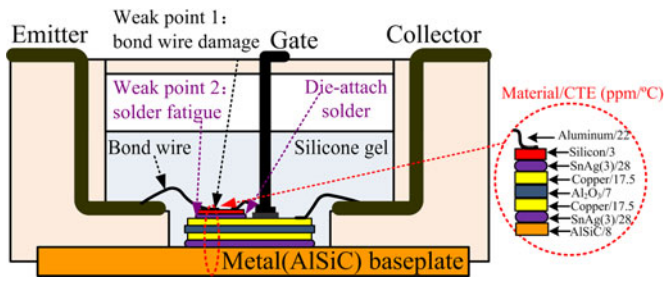

Fig. 3. Part of an IGBT module structure.

current going through the devices-under-test (DUTs) is always 100 mA, therefore, the measurement of V_{CE} will continually indicate the declining junction temperature [15]. Since the sensing current (100 mA) is significantly smaller than the controllable heating current (e.g., 40 A), it contributes little to the heating. This temperature-sensitive electrical parameter method has been proven [16]. The junction-to-case thermal resistance $R_{\rm th}$ of the module is computed at the beginning of each cooling phase from the junction-above-case temperature and the power loss which can be obtained from the voltage and current by the end of the heating-up phase. The test cycle lasts for at least 7 s, while the thermal time constant of the module is around 100 ms. The minimum junction temperature $(T_{j\min})$ is obtained in a similar way at the end of the cooling phase prior to the activation of the next heating-up phase. $(T_{j\max})$ and $(T_{j\min})$ define the stress level which can be adjusted by the duty ratio and period of the control switch. A small inductor is connected in the circuit to limit the current surge when the heating control switch turns ON.

B. Low ΔT_j Stress Cycle Test

Power modules are often used with ΔT_j up to 40 k. Therefore, it is important to understand the effect of the low ΔT_j stress cycles in lifetime modeling. Given the difficulty to wear out a new module, a staged test scheme is proposed for this purpose. Some new modules are first subjected to large ΔT_j cycles to cause initial solder cracks. Usually, once the thermal resistance

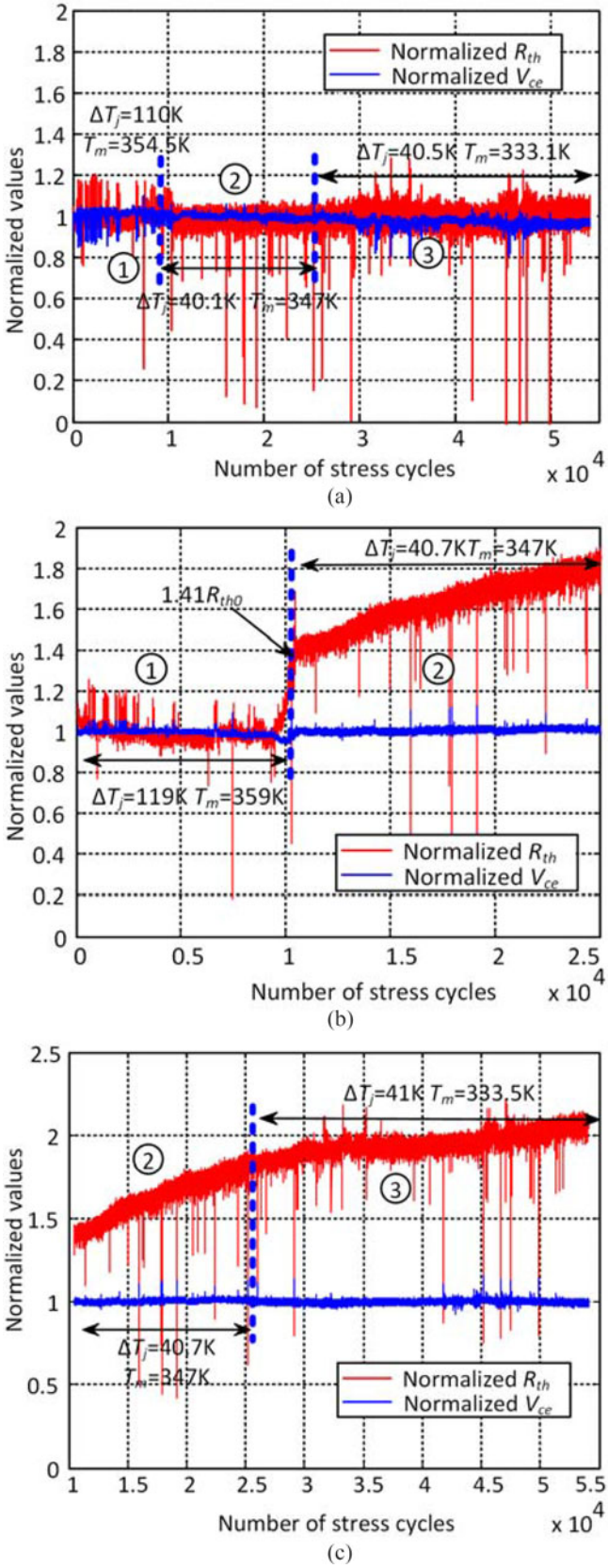

Fig. 4. Results of power cycling test. (a) Normalized $R_{\rm th}$ in an unaged module. (b) Normalized $R_{\rm th}$ for a new module under large ΔT_j and then small ΔT_j. (c) Normalized $R_{\rm th}$ in an aged module under small ΔT_j.

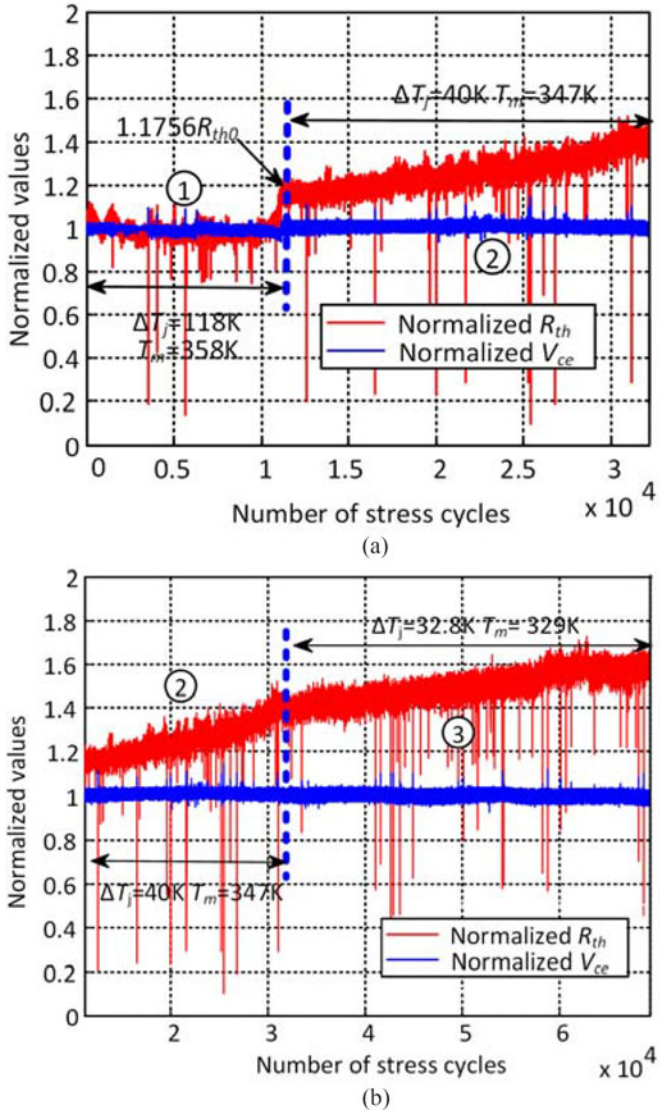

Fig. 5. Results of power cycling test. (a) Normalized $R_{\rm th}$ in a new module under large ΔT_j and then low ΔT_j. (b) Normalized $R_{\rm th}$ in aged module under low ΔT_j.

shows a noticeable increase, say 5% or more, the test condition is changed so that ΔT_j is reduced, while the mean junction temperature T_m is maintained at the target.

The first test aims to show qualitatively, the respective effects of ΔT_j, the mean junction temperature T_m and the present solder pad condition. Furthermore, change of $R_{\rm th}$ is monitored as the number of stress cycles increases; $R_{\rm th}$ is normalized with respect to its initial value for the new module: $R_{\rm th0}$. The DUT's normalized collector–emitter voltage under the heating current and $V_{\rm CE}$ with temperature compensation [13] are also included in the plot to make sure that a bond wire failure has not occurred, hence, the main ageing-to-failure mechanism under investigation is indeed the die-attach solder fatigue. Fig. 4 shows the test results.

Fig. 4(a) shows that, with different mean temperatures and $\Delta T_j \approx 40$ K in stages ②and ③ the condition of a nonaged

TABLE I
$R_{\rm th}$ AVERAGE INCREASE RATE UNDER DIFFERENT CONDITIONS

Test Conditions and $R_{\rm th}$ Increase Rate (per 1,000 cycles)			
$\Delta T_j = 40.7$ K, $T_m = 347$ K, $R_{\rm th} = 1.41 R_{\rm th0}$	2.9013%	$\Delta T_j = 41$ K, $T_m = 333.5$ K, $R_{\rm th} = 1.78\ R_{\rm th0}$	0.8001%
$\Delta T_j = 40$ K, $T_m = 347$ K, $R_{\rm th} = 1.18\ R_{\rm th}0$	1.1659%	$\Delta T_j = 32.5$ K, $T_m = 328.8$ K, $R_{\rm th} = 1.40 R_{\rm th0}$	0.5438%

TABLE II
TEST CONDITION OF MODULES

Sample module number and test stage number		$t_{\rm on}$	$t_{\rm off}$	ΔT_j	$T_{j\rm mean}$	Number of Cycles	I_c
Module 1	Stage ①	30 s	20 s	119 K	359 K	10461	60 A
	Stage ②	5 s	2 s	40.7 K	347 K	14825	45 A
	Stage ③	5 s	2 s	41 K	333.5 K	28790	40 A
Module 2	Stage ①	30 s	20 s	110 K	354.5 K	10461	60 A
	Stage ②	5 s	2 s	40.1 K	347 K	14825	45 A
	Stage ③	5 s	2 s	40.5 K	333.1 K	28790	40 A
Module 3	Stage ①	30 s	20 s	118 K	358 K	11136	60 A
	Stage ②	5 s	2 s	40 K	347 K	21007	45 A
	Stage ③	5 s	2 s	32.8 K	329 K	37306	40 A

module, measured by the junction-to-case thermal resistance $R_{\rm th}$, hardly changes. In Fig. 4(b), a brand new module is first subjected to a sufficient number of stress cycles with $\Delta T_j = 119$ K and $T_m = 359$ K to cause 40% increase of $R_{\rm th}$. The thermal resistance then continues to increase under $\Delta T_j \approx 40$ K and $T_m = 347$ K, which had no effect in Fig. 4(a). This is because once there is a crack in the solder layer, the stress close to the crack tip becomes greater than the overall average due to stress concentration; meanwhile, a plastic deformation zone is formed around the tip causing progressive degradation further. Therefore, it may be the case that low ΔT_j stress cycles should not be ignored for aged modules. Fig. 4(c) shows that the rate of further degradation also depends on the mean junction temperature, agreeing with the LESIT results [5].

This was confirmed in repeated tests. For instance, Fig. 5 shows the results when the thermal resistance is first increased to 1.1756 $R_{\rm th0}$ by accelerated ageing test. The effect of further low ΔT_j stress cycles is again observed but is reduced when compared to the previous results for the same ΔT_j and T_m on a more aged module. The ageing effect is still present when ΔT_j is reduced close to 30 K. From Figs. 4 and 5, the dependence of the $R_{\rm th}$'s rate of subsequent change on the severity of the stress cycles applied and the present health condition of the module is summarized in Table I, where the starting values of $R_{\rm th}$, 1.18 $R_{\rm th0}$, and 1.40 $R_{\rm th0}$, were obtained on two separate modules through different tests with intensified stress cycles. The test conditions are shown in Table II, where $t_{\rm on}$ is the heating-up phase time, $t_{\rm off}$ is the cooling phase time, and I_c is the heating current. The trend agrees with previous observations [17], as when the thermal resistance is larger and the crack is longer, the stress concentration effect will be stronger. On the other hand, the shear strength is inversely proportional to the crack length. The smaller the shear strength is, the more easily can the solder crack propagate.

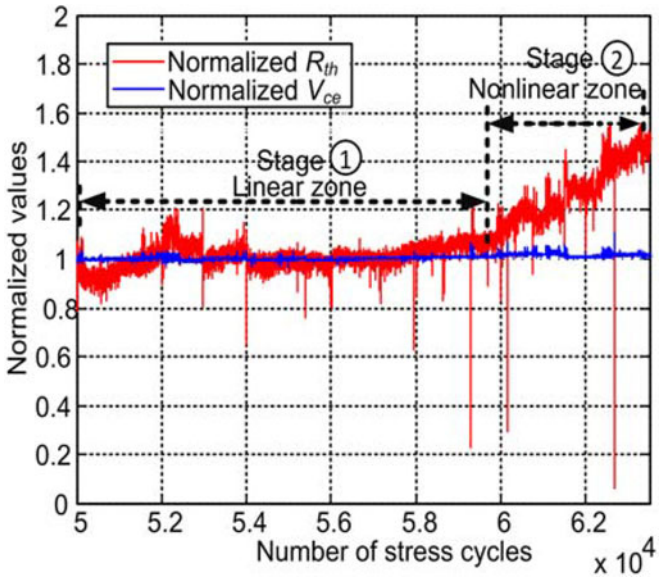

Fig. 6. Results of power cycling test with $\Delta T_j = 79$ K and $T_m = 354$ K.

In these preliminary tests, the modules were deliberately pushed into a high degree of damage in order to capture the effect of the low ΔT_j stress cycles. Gachovska *et al.* suggested that a 20% increase of the thermal resistance signifies solder fatigue [18]. Some other studies indicated that a 50% increase may be a more appropriate inflection point [13]. The later tests which are used in this paper to extract the parameters of the lifetime model will cover the damage in the commonly used range from 1% to 20% increase of $R_{\rm th}$.

III. ASSUMPTION AND MODEL STRUCTURE

Fig. 6 shows the overall profile of the module junction-to-case thermal resistance $R_{\rm th}$, increasing with the number of stress cycles in an accelerated test with roughly constant ΔT_j and T_m. From the device health condition point of view, the ageing process can be divided into two stages. It is assumed that the first stage includes fatigue and creep wear-out, which is progressive structural damage caused by repeated oscillating stress below the yield point of the material. The process starts with dislocation movements, forming persistent slip bands that behave as nucleate microscopic cracks. It would take many minor stress cycles to exhaust the first stage, and the condition cannot be detected through $R_{\rm th}$. From a practical point of view, in many engineering systems, during such a long time it is likely that more severe stress cycles will occur pushing the lifetime consumption into the second stage. It is further assumed that in the second stage, macroscopic cracks have been initiated and this will be followed by incremental crack propagation leading to the final failure. The effects of all stress cycles are increased in this stage and this is the dominant mechanism considered here for the minor stress cycles to contribute to the consumption of the module lifetime. Ageing develops faster because both

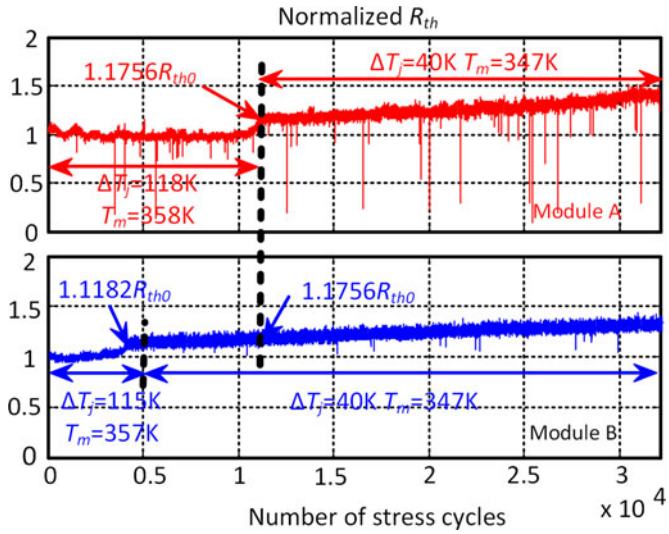

Fig. 7. Comparing the change of the thermal resistance for two modules.

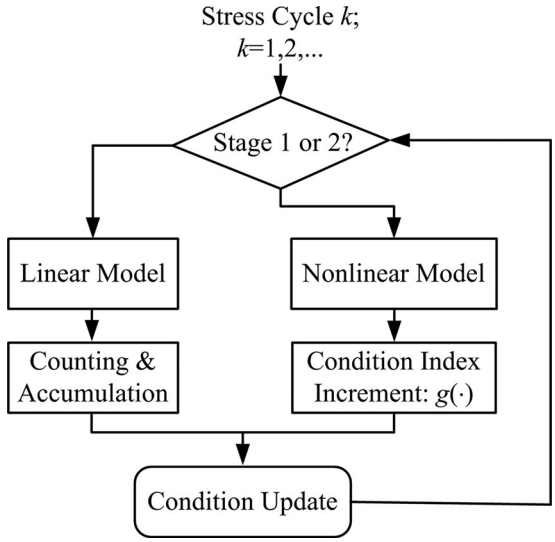

Fig. 8. Structure of the proposed model.

severe and minor stress cycles will now have more significant effect. The first stage is referred to as the linear and second as the nonlinear stage. In the linear stage, the effects of different stress cycles can be added by superimposition according to Miner's rule, while the effects themselves are estimated using a Coffin–Manson–Arrhenius model to account for the different values of ΔT_j and T_m [9], [19].

This study intends to develop a lifetime model mainly for condition monitoring of converters with power modules in the second stage. The change of $R_{\rm th}$ needs to be detected and Fig. 6 implies that there will be a period of time after a noticeable $R_{\rm th}$ increase and before the complete failure. This allows maintenance scheduling. In the design of some highly reliable systems, it is possible to require that no noticeable $R_{\rm th}$ increase should be caused during the entire life expectation. This study does not focus on the low ΔT_j stress cycle effect in the first stage, during which the traditional linear extrapolation and superimposition model is still used.

A key assumption made to establish the lifetime model is that the health condition of the power module, in terms of solder fatigue, can be measured by the junction-to-case thermal resistance, $R_{\rm th}$. The operational history for the module to reach the present health condition $R_{\rm th}$ has no further effect.

Fig. 7 shows the further increase of $R_{\rm th}$ in the nonlinear stage of two IGBT modules of the same type starting from almost the same health condition ($R_{\rm th} \approx 1.176\ R_{\rm th0}$) reached through two different routes. It seems that the future rate of change of $R_{\rm th}$ is independent of the past history of ageing. For further stress cycles of $\Delta T_j \approx 40$ K and $T_m \approx 347$ K, the rate of change is 0.71978% every 1000 cycles for Module A and 0.71408% every 1000 cycles for Module B. The further development of ageing is indeed very similar for both modules. These results to some extent confirm the assumption made in this study.

Fig. 8 shows the structure of the proposed lifetime model, divided into two corresponding stages. Ageing develops in the first, linear stage but is not measurable in $R_{\rm th}$. The effect of the minor stress cycles is only considered in the nonlinear stage assuming that only elastic deformation is present in this stage. This depends on the current health condition of the module measured in $R_{\rm th}$ in addition to the intensity of the stress itself which is defined in terms of ΔT_j and the mean junction temperature T_m. The core part of the model is the function to estimate the incremental effect of a stress cycle: g ($R_{\rm th}$, ΔT_j, T_m). In real-time applications, where the model is used to estimate the remaining lifetime for a given future mission profile, the module health condition can be measured and dynamically updated. A deterministic approach is described here due to limitations of resources but the idea can be extended to include the statistical nature of the ageing effect.

Once the measured or calculated junction-to-case thermal resistance $R_{\rm th}$ is constantly above a preset value, say 0.5% increase from the initial value, the damage accumulation model is considered to be in the nonlinear stage, and the further increase of the thermal resistance is no longer, on a large scale, proportional to the number of the stress cycles even the severity of each cycle is the same. The ageing process generally develops progressively faster. This means that the sequence in which different stress cycles occur would affect their ageing consequence.

IV. Die-Attach Solder Fatigue Lifetime Model

Existing lifetime models to evaluate the effect of stress cycles are in general of two types: 1) analytical behavior models such as the Coffin–Manson [8], Norris–Landzberg [20], and Bayerer models [21], and 2) physics-of-failure models [17], [22]. This paper describes the work adopting the analytical approach. All the models were previously established from large ΔT_j tests (power or temperature cycling), without directly confirming small ΔT_j effect. This study intends to provide the evidence of small ΔT_j effect and propose a model to represent such effect for lifetime evaluation. For power modules of silicon-based devices, by large ΔT_j, it generally means the temperature

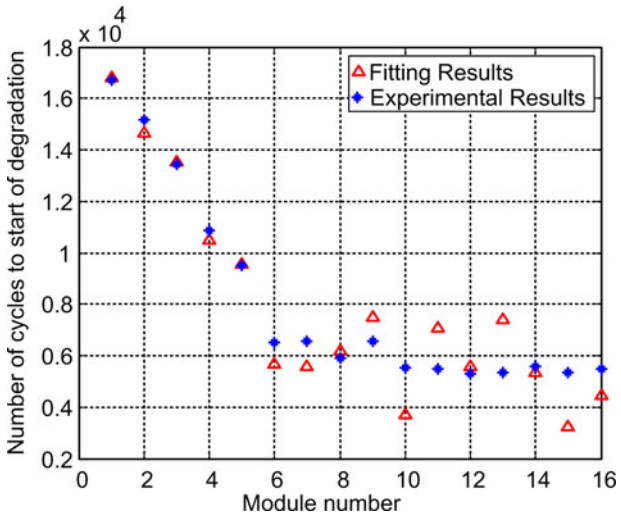

Fig. 9. Fitting results of the Coffin–Manson–Arrhenius model.

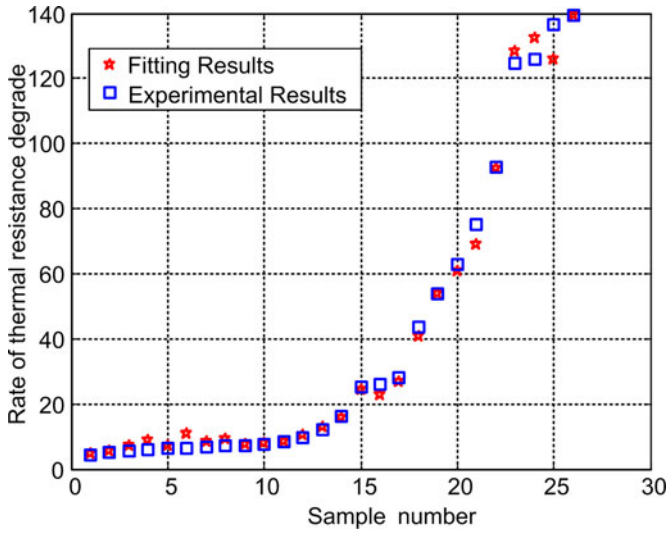

Fig. 10. Function fitting result.

variation range that can be used in accelerated lifetime testing, e.g., 80–120 K. In a practical converter, conditions close to this range could be encountered in extreme cases or during transients. By small ΔT_j, it means the temperature variation range expected during the normal steady-state operation, e.g., 40 K. In addition to ΔT_j, the mean junction temperature T_m is also an important variable. As ΔT_j and T_m are decided by different factors in the converter operation, they are treated as independent variables in model derivation.

A. Linear Accumulation Model

According to Miner's rule when the module is under cyclic loading with a mixture of different amplitudes [23], the accumulative damage D can be calculated from (1), where $N(i)$ is the total number of cycles at the ith amplitude and $N_c(i)$ is the number of cycles at that amplitude to fully consume the linear stage [24]. It is arbitrarily assumed that the linear stage finishes when the accumulative damage (mean value) is consistently 0.5% of the total damage to failure. The most important characteristic is the load sequence independence of Miner's rule

$$D = 0.005 \cdot \sum_i N(i)/N_c(i). \tag{1}$$

B. Coffin–Manson–Arrhenius Model

Die-attach solder fatigue is mainly attributed to the thermomechanical effect caused by repeated flexure of the shear stress between the die and solder layer. A Coffin–Manson model defines a power law relationship between the numbers of cycles N_c [corresponding to that in (1)] and ΔT_j [8], further taking into account the mean junction temperature T_m. Here, the mean junction temperature is assumed to have a simple thermally activated mechanism which is enhanced at escalated temperatures according to Arrhenius' law [9], [25].

This is shown in (2) which is only used for the linear stage. Function fitting is used to obtain the model parameters as shown in Fig. 9. From the test results ($\Delta T_j \geq 114$ K) on 16 sample

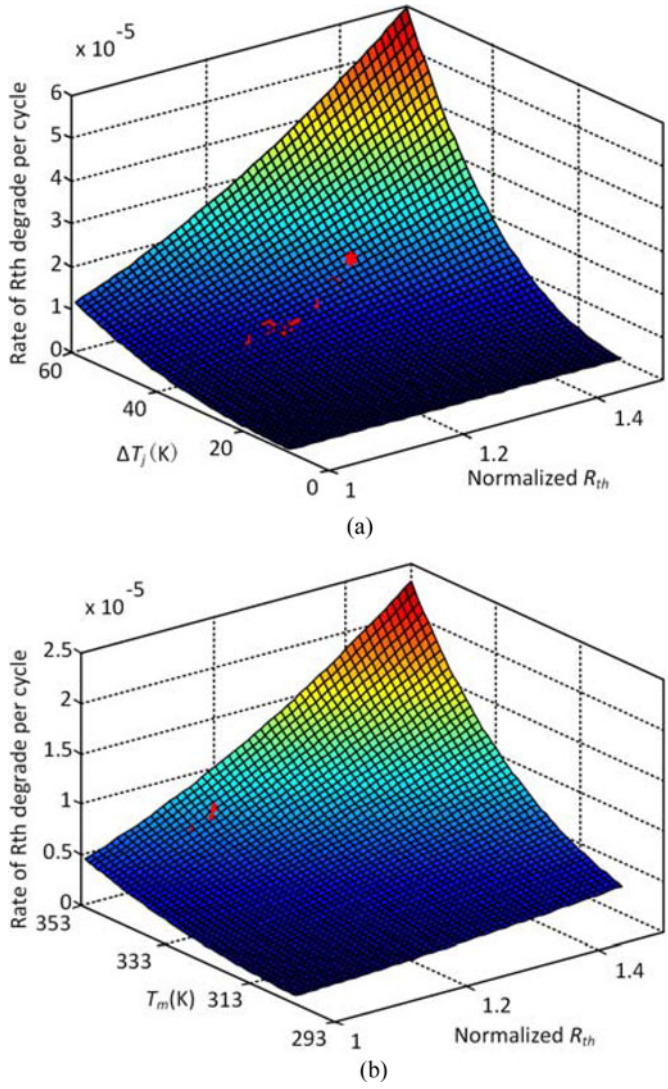

Fig. 11. R in different conditions. (a) $T_m = 348$ K. (b) $\Delta T_j = 40$ K.

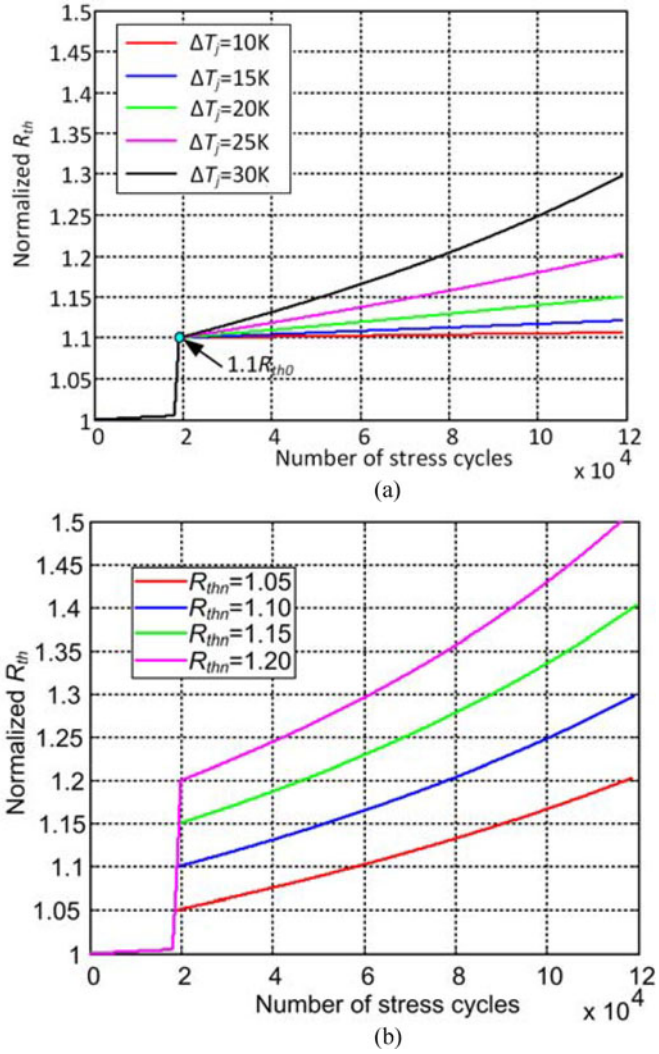

Fig. 12. $R_{\rm th}$ in different conditions. (a) Nonlinear growth of $R_{\rm th}$ with different stress cycles (T_m = 333 K). (b) Nonlinear growth of $R_{\rm th}$ from different $R_{\rm th}$ (ΔT_j = 30 K, T_m = 333 K).

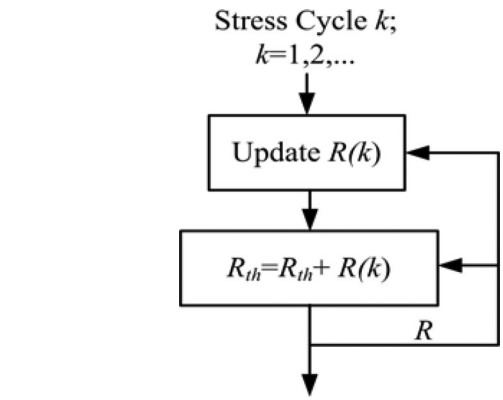

Fig. 13. Block diagram of the accumulative damage model in the nonlinear stage.

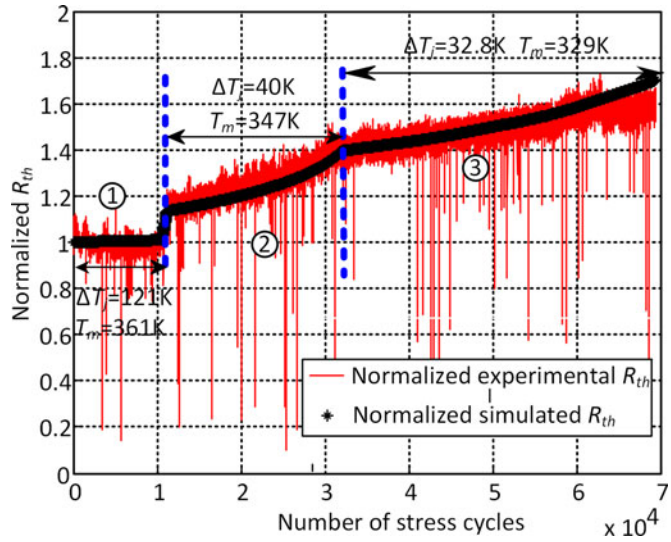

Fig. 14. Simulation and experimental results.

modules of the same type, model parameters A_1, α, and A_2 are found to be 3.71×10^{13}, -10.122, and 9445.52, respectively. Pearson's correlation coefficient is calculated to check the function fitting strength, and the correlation coefficient is 0.9618 which implies a strong correlation

$$N_c = A_1 \cdot (\Delta T_j)^{\alpha} \cdot e^{(\frac{A_2}{T_m})}. \tag{2}$$

C. Nonlinear Accumulation Model

The rate of change of $R_{\rm th}$ with respect to the number of stress cycles is extracted from tests under a range of conditions in terms of ΔT_j, T_m, and the present value of the normalized $R_{\rm th}$. In the nonlinear stage, it is now possible to measure the effect of minor stress cycles by the experiment because the effect can be observed within a realistic number of cycles. The impact of the mean junction temperature on the degradation rate can usually be represented by an Arrhenius law model [26] and an exponential function can be used to express the stress concentration effect [27]. A model is proposed as shown below in (3), where R is the rate of increase of the normalized thermal resistance $R_{\rm th}$ (1/cycle) depending on $\Delta T_j, T_m$ and $R_{\rm th}$. A higher junction temperature increases the thermo-mechanical stresses, due to the exacerbation of mismatch of thermal expansion between the die and solder. Larger thermal resistance means that the total crack length has grown and the stress concentration effect is consequently stronger. These imply that $b_2 < 0, b_3 > 0$, and $\ln(b_4 \cdot R_{\rm thn}) + b_5(R_{\rm thn})^{b6} > 0$. Function fitting is again resorted to obtain the parameters as shown in Fig. 10 using 26 sampling points and tests carried out in the range of 30 K $\leq\Delta T_j\leq$120 K, 330 K$\leq T_m \leq$362 K, and $1.01 \leq R_{\rm th} \leq 1.50$, on four modules of the same type which are already in the nonlinear stage. The rate of $R_{\rm th}$ increase is measured over a few (e.g., 1000) stress cycles. Because the number of stress cycles is small, the rate can be measured based on linearization. The parameters derived are: $b_1 = 706.1824$, $b_2 = -4656.0962$, $b_3 = 2.7835$, $b_4 = 3.78811$, $b_5 = -3.4773$, and $b_6 = -1.1005$. Pearson's correlation coefficient of determination is calculated to check the fitting strength, and the correlation coefficient is

TABLE III
ERRORS OF SIMULATED $R_{\rm th}$ UNDER DIFFERENT CONDITIONS

Sample module number and stage number		ΔT_j	T_m	$R_{\rm th}$ error at the end of stage, for simulation from beginning ($R_{\rm th} = 1.0R_{\rm th0}$)	$R_{\rm th}$ error at the end of stage, for simulation from $R_{\rm th} = 1.005R_{\rm th0}$
Module 1	Stage ①	119 K	359 K	9.2120%	1.3967%
	Stage ②	40.7 K	347 K	12.933%	1.2733%
	Stage ③	-	-	*	*
Module 2	Stage ①	113 K	359 K	2.6755%	2.6765%
	Stage ②	32.8 K	329 K	4.0493%	4.0469%
	Stage ③	40 K	347.5 K	3.9969%	3.9933%
Module 3	Stage ①	118 K	358 K	3.5536%	3.5301%
	Stage ②	40 K	347 K	0.0086%	0.0086%
	Stage ③	32.8 K	329 K	6.3840%	6.1657%
Module4	Stage ①	115 K	357 K	0.6163%	0.6171%
	Stage ②	40 K	347 K	2.7210%	2.7159%
	Stage ③	-	-	*	*

*test results unavailable

0.9978, confirming that the model can be confidently used for calculating *R*. The variation of *R* is calculated for different conditions to illustrate the effects of $\Delta T_j, T_m$, and $R_{\rm th}$ as shown in Fig. 11. As the normalized $R_{\rm th}$ is reduced to 1.0, the rate of change *R* is reduced to zero corresponding to the linear stage of the ageing process

$$R = b_1 \cdot e^{\left(\frac{b_2}{T_m}\right)} \cdot (\Delta T_j)^{b_3} \cdot e^{(\ln(b_4 \cdot R_{\rm th}) + b_5 \cdot (R_{\rm th})^{b_6})}. \quad (3)$$

Fig. 12 presents a series of computational results of the thermal resistance $R_{\rm th}$ based on (3) to illustrate the growth of $R_{\rm th}$ in the nonlinear stage, as affected by ΔT_j, T_m, and $R_{\rm th}$ in the second stage of the simulated ageing process. It is assumed that for each curve, stress cycles remain the same. The effects of the stress and module initial conditions are obvious and the increase of $R_{\rm th}$ in all cases is indeed nonlinear. The updated $R_{\rm th}$ is the sum of the current value and the multiplication of *R* with $N_{\rm cycle}$, where the $N_{\rm cycle}$ is the number of stress cycles and *R* is the rate of $R_{\rm th}$ increase for the corresponding stress level.

D. Summary and Validation: The Damage Accumulation Model

It is expected that the model structure can be applied to all IGBT power modules but the model parameters should be extracted for each type of design because designs can differ in die size, packaging structure, and material which will affect the details of the model. The lifetime of a power module is to be consumed in two sequential stages: 1) the linear stage during which the thermal resistance (mean value) does not obviously change, and 2) the nonlinear stage during which the thermal resistance changes with the stress cycles experienced by the module. In line with the model structure of Fig. 8, the procedure to estimate the accumulative damage is described as follows. The stress cycles are grouped into different types. Each type (each *i*) corresponds to certain ΔT_j and T_m.

1) In the linear stage, the total effect of a type of stress cycles depends on the intensity and number of the cycles. It is independent of the health condition of the module because the effect of each additional stress cycle is only a small increment. It is arbitrarily assumed that at the end of the linear stage, the normalized thermal resistance (mean value) is increased by 0.5%. The algorithm to calculate the accumulative damage $\Delta R_{\rm th}$ of all types of stress cycles is described in (4) and (5), based on linear superimposition

$$\Delta R_{\rm th} = 0.005 \sum_i \frac{N(i)}{N_c(i)}. \quad (4)$$

$$N_c(i) = A_1 \cdot [\Delta T_j(i)]^{\alpha} \cdot e^{\left[\frac{A_2}{T_m(i)}\right]}. \quad (5)$$

where *N*(*i*) is the number of stress cycles of type *i*; $N_c(i)$ is the number of stress cycles of type *i* which increases the thermal resistance by 0.5%. A_1, α, and A_2 are the parameters which have been derived from experiments.

2) When $R_{\rm th}$ increased over 0.5%, the module ageing process entered the nonlinear stage. Because the rate of $R_{\rm th}$ growth, *R*, in this stage will depend on the normalized thermal resistance itself, the accumulative damage (measured by the increasing thermal resistance) has to be calculated by accumulation in a sequence to take into account all the stress cycles. *R* is updated in the process using (3). The calculation is shown in Fig. 13.

The test results of four sample modules have been used to extract parameters of the lifetime model for the nonlinear stage. Twelve additional modules have been used for the linear stage because of the difficulty to precisely capture the number of stress cycles causing 0.5% increase of $R_{\rm th}$. Once the model is obtained, the temperature cycling profiles of individual modules can be input into the model to simulate the increase of $R_{\rm th}$ from the initial condition. Because the actual temperature profile is somewhat different from module to module due to their locations on the test rig, their ageing processes can also differ. Fig. 14 compares the measured and simulated $R_{\rm th}$ for Module 3 in the original arrangement. Good agreement is observed over the entire test duration. However, bigger discrepancies have been observed for some other modules. Table III summarizes the errors of estimating the thermal resistance reached by the end of the three test stages as shown in Fig. 14, showing the statistic deviation between the modules, which is also evident in Figs. 9 and 10. The error is 9.212% for Module 1 by the end of test stage ① While the error is comparable to what was found in the past [5], [13], it can be carried to further predictions and can get amplified because of the dependence of the rate of $R_{\rm th}$ increase R on the current health condition which is measured by $R_{\rm th}$. However, if the future prediction in the nonlinear stage is set to start from a measured value of the increased thermal resistance, the error from the linear stage will not be carried into the nonlinear stage which can then be more accurately predicted. The final column in Table III shows clearly the improved accuracy of onward simulations after $R_{\rm th}$ is detected to have increased by 1%. This is practically using the part of the lifetime model for the second, nonlinear stage only.

For this reason, the lifetime model including both the linear and nonlinear stages is not recommended for design studies where it is important to accurately predict the stress effect in the linear stage. The authors are confident that the model can accurately estimate the effect of low (and large) ΔT_j stress cycles in the nonlinear stage of the ageing process as long as the function of rate of $R_{\rm th}$ increase can be accurately extracted as shown in Fig. 10. Therefore, the proposed lifetime model could be suitably used to support condition monitoring and prognosis in operational management. The health condition indicator $R_{\rm th}$ can be monitored from measurements external to the module packaging [28] and the result can be used to estimate the remaining lifetime.

It is noted that in the design of some highly reliable power electronic systems, such as converters in aerospace servo drives, it is not permitted for the power module to show any degradation of the health condition. Accurate modeling of the linear stage of the ageing process then becomes extremely important. Creep wear-out mechanisms should be more precisely understood. Investigations assisted by microscopy and FEA modeling would be required to further the knowledge. But, this is currently beyond the ability of the authors.

A further validation test has been carried out as shown in Fig. 15. The SKM50GB12T4 module under test is a brand new module and the test results have not been used to extract the model parameters. The stress cycles applied are also different to the previous tests. Fig. 15(a) shows that the model results agree well with the test results. Fig. 15(b) shows the profiles of the maximum and minimum junction temperatures during the entire test span. It happens that the simulated $R_{\rm th}$ value by the end of test stage ①is close to the measurement.

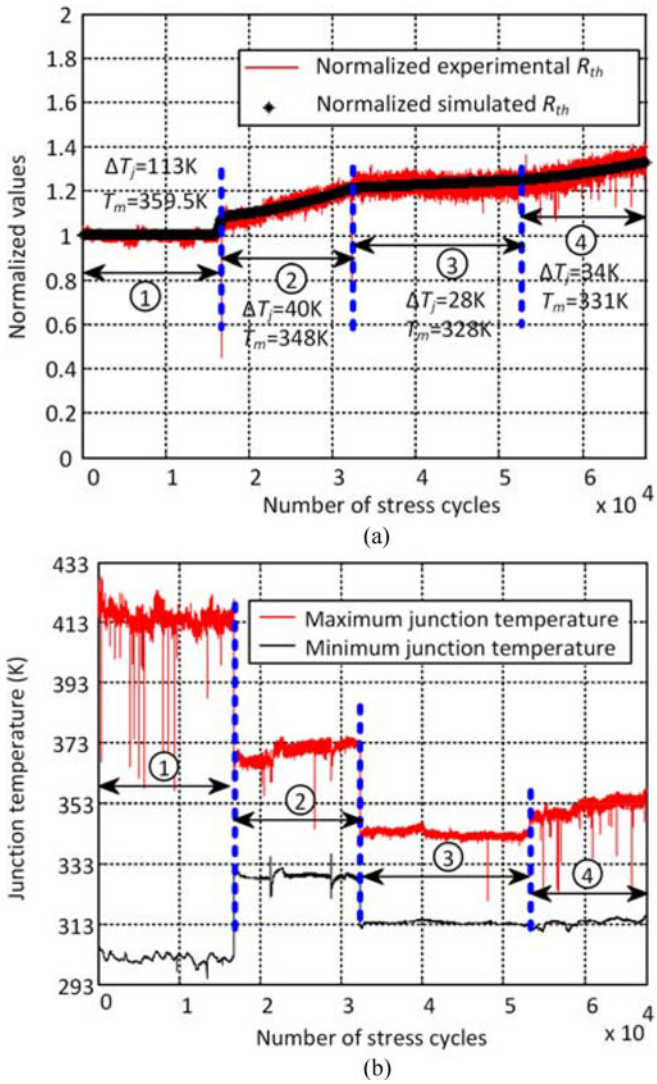

Fig. 15. Simulation and experiment results. (a) Normalized thermal resistance. (b) Junction temperature profiles.

V. Conclusion

This paper summarizes the main findings of an investigation on the lifetime effect of relatively minor stress cycles that are expected during normal operation of many power electronic systems. It is unrealistic to carry out cycling-to-failure tests in such conditions and the results, if obtained, would be highly questionable. The ageing process is divided into two sequential stages: the linear and nonlinear stages. These minor stress cycles may contribute only slightly to the lifetime consumption in the linear stage, but their effects are mostly manifested in the nonlinear stage. Testing on aged modules allows the effect to be observed and modeled. A model is established to estimate the rate of increase of the junction-to-case thermal resistance which is normalized and adopted to measure the health condition. It is confirmed that the rate of increase of the thermal resistance depends on not only the nature of the stress cycle (ΔT_j and T_m), but also the present health condition itself. A new lifetime model is proposed to represent the effect of each stress cycle and the accumulative effect of consecutive cycles. Experiments verify the new lifetime model. It is hoped that the study would help developing condition-monitoring-based operational management strategies for converter systems that are expected to operate reliably over a long time subjected to a large number of minor stress cycles. It is also hoped that future work could lead to more accurate modeling of such stress cycles in the linear stage of the ageing process, resulting in a lifetime model that can more effectively support converter design studies.

References

[1] S. Yang, A. T. Bryant, P. A. Mawby, D. Xiang, L. Ran, and P. Tavner, "An industry-based survey of reliability in power electronic converters," in *Proc. Energy Convers. Congr. Expo.*, San Jose, CA, USA, 2009, pp. 1441–1451.

[2] E. Wolfgang, "Examples for failures in power electronics systems," presented at *ECPE Tutorial on Reliability of Power Electronic Systems*, Nuremberg, Germany, Apr. 2007.

[3] *Handbook for Robustness Validation of Automotive Electrical/Electronic Modules*, Zentralverband Elektrotechnik-und Elektronikindustrie, Frankfurt, Germany, Jun. 2008.

[4] H. Wang, K. Ma, and F. Blaabjerg, "Design for reliability of power electronic systems," in *Proc. IEEE Ind. Electron. Soc.*, 2012, pp. 33–44.

[5] M. Held, P. Jacob, G. Nicoletti, P. Scacco, and M. H. Poech, "Fast power cycling test for IGBT modules in traction application," *IEEE Int. Conf. Power Electron. Drive Syst.*, 1997, vol. 1, pp. 425–430.

[6] R. Jones and P. Waite, "Optimised converter for multi-MW direct drive permanent magnet wind turbines," presented at the *14th Eur. Conf. Power Electron. Appl.*, Birmingham, U.K., 2011.

[7] K. Ma, M. Liserre, and F. Blaabjerg, "Lifetime estimation for the power semiconductors considering mission profiles in wind power converter," in *Proc. IEEE Energy Convers. Congr. Expo.*, Sep. 15–19, 2013, pp. 2962–2971.
[8] C. Busca, R. Teodorescu, F. Blaabjerg, S. Munk-Nielsen, L. Helle, T. Abeyasekera, and P. Rodriguez, "An overview of the reliability prediction related aspects of high power IGBTs in wind power applications," *Microelectron. Rel.*, vol. 51, no. 9–11, pp. 1903–1907, Sep.–Nov. 2011.
[9] S. Yang; D. Xiang, A. Bryant, P. Mawby, L. Ran, and P. Tavner, "Condition monitoring for device reliability in power electronic converters: A review," *IEEE Trans. Power Electron.*, vol. 25, no. 11, pp. 2734–2752, Nov. 2010.
[10] M. Ciappa, "Selected failure mechanisms of modern power modules," *Microelectron. Rel.*, vol. 42, no. 4, pp. 653–667, Apr. 2002.
[11] D. C. Katsis and J. D. Van Wyk, "Void-induced thermal impedance in power semiconductor modules: some transient temperature effects," *IEEE Trans. Ind. Appl.*, vol. 39, no. 5, pp. 1239–1246, Sep. 2003.
[12] P. Ratchev, B. Vandevelde, and I. De Wolf, "Reliability and failure analysis of Sn-Ag-Cu solder interconnections for PSGA packages on Ni/Au surface finish," *IEEE Trans. Device Mater. Rel.*, vol. 4, no. 1, pp. 5–10, Mar. 2004.
[13] H. Huang and P. A. Mawby, "A lifetime estimation technique for voltage source inverters," *IEEE Trans. Power Electron.*, vol. 28, no. 8, pp. 4113–4119, Aug. 2013.
[14] A. Morozumi, K. Yamada, T. Miyasaka, S. Sumi, and Y. Seki, "Reliability of power cycling for IGBT power semiconductor modules," *IEEE Trans. Ind. Appl.*, vol. 39, no. 3, pp. 665–671, May–Jun. 2003.
[15] H. Chen, B. Ji, V. Pickert, and W. Cao, "Real-time temperature estimation for power MOSFETs considering thermal aging effects," *IEEE Trans. Device Mater. Rel.*, vol. 14, no. 1, pp. 220–228, Mar. 2014.
[16] B. Ji, V. Pickert, W. Cao, and B. Zahawi, "In situ diagnostics and prognostics of wire bonding faults in IGBT modules for electric vehicle drives," *IEEE Trans. Power Electron.*, vol. 28, no. 12, pp. 5568–5577, Dec. 2013.
[17] L. Yang, P.A. Agyakwa, and C. M. Johnson, "Physics-of-failure lifetime prediction models for wire bond interconnects in power electronic modules," *IEEE Trans. Device Mater. Rel.*, vol. 13, no. 1, pp. 9–17, Mar. 2013.
[18] T. K. Gachovska, T. Bo, J. Hudgins, Q. Wei, and J. Donlon, "A real-time thermal model for monitoring of power semiconductor devices," in *Proc. IEEE Energy Convers. Congr. Expo.*, Sep. 15–19, 2013, pp. 2208–2213.
[19] L. R. GopiReddy, L. M. Tolbert, B. Ozpineci, and J. Pinto, "Rainflow algorithm based lifetime estimation of power semiconductors in utility applications," *IEEE Trans. Ind. Appl.*, vol. 51, no. 4, pp. 3368–3375, Feb. 2015.
[20] I. F. Kovacevic, U. Drofenik, and J. W. Kolar, "New physical model for lifetime estimation of power modules," in *Proc. Int. Power Electron. Conf.*, 2010, pp. 2106–2114.
[21] R. Bayerer, T. Hermann, T. Licht, J. Lutz, and M. Feller, "Model for power cycling lifetime of IGBT modules–various factors influencing lifetime," presented at the *5th Int. Conf. Integr. Power Electron. Syst.*, Nuremberg, Germany, Mar. 11–13, 2008.
[22] G. Khatibi, M. Lederer, B. Weiss, T. Licht, J. Bernardi, and H. Danninger, "Accelerated mechanical fatigue testing and lifetime of interconnects in micro-electronics," *Proc. Eng.*, vol. 2, no. 1, pp. 511–519, Apr. 2010.
[23] C. Y. Yin, H. Lu, M. Musallam, C. Bailey, and C. M. Johnson, "A physics-of-failure based prognostic method for power modules," in *Proc. 10th Electron. Packag. Technol. Conf.*, Dec. 9–12, 2008, pp. 1190–1195.
[24] L. Yang, L. Yin, B. Arafei, B. Roggeman, and P. Borgesen, "On the assessment of the life of SnAgCu solder joints in cycling with varying amplitudes," *IEEE Trans. Compon., Packag. Manuf. Technol.*, vol. 3, no. 3, pp. 430–440, Mar. 2013.
[25] H. Cui, "Accelerated temperature cycle test and Coffin–Manson model for electronic packaging," in *Proc. Annu. Rel. Maintainability Symp.*, 2005, pp. 556–60.
[26] J. W. McPherson, *Reliability Physics Engineering: Time-to-Failure Modeling*, Second 2nd ed. New York, NY, USA: Springer, 2013, pp. 104–106.
[27] L. Yang, P. A. Agyakwa, and C. M. Johnson, "A time-domain physics-of-failure model for the lifetime prediction of wire bond interconnects," presented at the *European Symposium on Reliability of Electron Devices, Failure Physics and Analysis*, Bordeaux, France, vol. 51, 2011.
[28] D. Xiang, L. Ran, P. J. Tavner, A. Bryant, S. Yang, and P. A. Mawby, "Monitoring solder fatigue in a power module using case-above-ambient temperature rise," *IEEE Trans. Ind. Appl.*, vol. 47, no. 6, pp. 2578–2591, Nov./Dec. 2011.

Wei Lai received the M.Sc. degree from the Chongqing University of Technology, Chongqing, China, in 2012. He is currently working toward the Ph.D. degree in electrical engineering in the School of Electrical Engineering, Chongqing University, Chongqing.

He was a joint Ph.D. student funded by the China Scholarship Council at the University of Warwick, Coventry, U.K., from September 2013 to May 2015. His research interests include the reliability of power modules, the application of power electronics for electric power generation, and the development of condition monitoring methods for power electronic converters.

Minyou Chen (M'05–SM'14) received the M.Sc. degree in control theory and engineering from Chongqing University, Chongqing, China, in 1987, and the Ph.D. degree in control engineering from the University of Sheffield, Sheffield, U.K., in 1998.

He is currently a Full Professor at Chongqing University. He is the author or coauthor of more than 180 papers. His research interests include intelligent modeling and control, reliability of power modules, microgrid control, and state monitoring in power distribution systems.

Li Ran (M'98–SM'07) received the Ph.D. degree in power systems engineering from Chongqing University, Chongqing, China, in 1989.

He was a Research Associate with the Universities of Aberdeen, Nottingham, and Heriot-Watt, at Aberdeen, Nottingham, and Edinburgh, U.K., respectively. He became a Lecturer of power electronics at Northumbria University, Newcastle upon Tyne, U.K., in 1999, and was seconded to Alstom Power Conversion, Kidsgrove, U.K., in 2001. Between 2003 and 2012, he was with Durham University, U.K. He joined the University of Warwick, Coventry, U.K., as a Professor in power electronics systems in 2012. His research interests include the application of power electronics for electric power generation, delivery, and utilization.

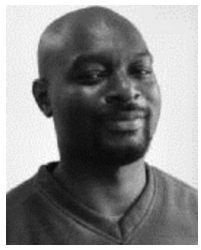

Olayiwola Alatise (M'05) received the B.Eng. degree (first-class Hons.) in electronic engineering and the Ph.D. degree in microelectronics and semiconductors from Newcastle University, Newcastle upon Tyne, U.K., in 2005 and 2008, respectively.

His research focused on mixed-signal performance enhancements in strained Si/SiGe metal–oxide–semiconductor field-effect transistors (MOSFETs). In June 2008, he joined the Innovation R&D Department, NXP Semiconductors, as a Development Engineer, where he designed, processed, and qualified discrete power trench MOSFETs for automotive applications and switched-mode power supplies. In November 2010, he became a Science City Research Fellow at the University of Warwick, Coventry, U.K., where he has been serving as an Associate Professor of electrical engineering since August 2012. His research interests include investigating advanced power semiconductor materials and devices for improved energy conversion efficiency.

Shengyou Xu received the Ph.D. degree in electrical engineering from Chongqing University, Chongqing, China, in 2013.

He was a Visiting Scholar at Durham University, Durham, U.K., in 2010. He is currently a Lecturer of electrical engineering at the School of Electrical Engineering, Chongqing University. His research interests include the control of power system and the reliability of power module used in renewable energy systems.

Philip Mawby (S'85–M'86–SM'01) received the B.Sc. and Ph.D. degrees in electronic and electrical engineering from the University of Leeds, Leeds, U.K., in 1983 and 1987, respectively.

His Ph.D. research was focused on GaAs/AlGaAs heterojunction bipolar transistors for high-power radio frequency applications at the GEC Hirst Research Centre, Wembley, U.K. In 2005, he joined the University of Warwick, Coventry, U.K., as the Chair of power electronics. He was also with the University of Wales, Swansea, U.K. for 19 years and held the Royal Academy of Engineering Chair for power electronics, where he established the Power Electronics Design Center. He has been internationally recognized in the area of power electronics and power device research. He was also involved in the development of device simulation algorithms, as well as optoelectronic- and quantum-based device structures. He has authored or coauthored more than 100 journal and conference papers. His current research interests include materials for new power devices, and modeling of power devices and circuits.

He has been involved in many international conference committees, including the International Symposium on Power Semiconductor Devices and ICs, the European Power Electronics, and the European Solid-State Device Conference. He is a Chartered Engineer. He is a Distinguished Lecturer for the IEEE Electron Devices Society.

Dr. Mawby is a Fellow of the Institution of Engineering and Technology and the Institute of Physics.